

Université Libre de Bruxelles

*Institut de Recherches Interdisciplinaires
et de Développements en Intelligence Artificielle*

**Operational aspects of the evolved
signalling behaviour in a group of
cooperating and communicating robots**

Elio TUCI, Christos AMPATZIS, Federico VICENTINI, and
Marco DORIGO

IRIDIA – Technical Report Series

Technical Report No.
TR/IRIDIA/2006-016

May 2006

IRIDIA – Technical Report Series
ISSN 1781-3794

Published by:

IRIDIA, *Institut de Recherches Interdisciplinaires
et de Développements en Intelligence Artificielle*
UNIVERSITÉ LIBRE DE BRUXELLES
Av F. D. Roosevelt 50, CP 194/6
1050 Bruxelles, Belgium

Technical report number TR/IRIDIA/2006-016

Revision history:

TR/IRIDIA/2006-016.001 May 2006
TR/IRIDIA/2006-016.002 July 2006

The information provided is the sole responsibility of the authors and does not necessarily reflect the opinion of the members of IRIDIA. The authors take full responsibility for any copyright breaches that may result from publication of this paper in the IRIDIA – Technical Report Series. IRIDIA is not responsible for any use that might be made of data appearing in this publication.

Operational aspects of the evolved signalling behaviour in a group of cooperating and communicating robots

Elio TUCI[‡] etuci@ulb.ac.be

Christos AMPATZIS[‡] campatzi@ulb.ac.be

Federico VICENTINI[†] federico.vicentini@polimi.it

Marco DORIGO[‡] mdorigo@ulb.ac.be

[‡] IRIDIA, CoDE, Université Libre de Bruxelles, Bruxelles, Belgium

[†] Robotics Lab, Mechanics Dept., Politecnico di Milano, Milano, Italy

May 2006

Abstract

This paper complements the results and analysis shown in current studies on the evolution of signalling and cooperation. It describes operational aspects of the evolved behaviour of a group of robots equipped with a different set of sensors, that navigates towards a target in a walled arena. In particular, analysis of the sound signalling behaviour shows that the robots employ the sound to remain close to each other at a safe distance with respect to the risk of collisions. Spatial discrimination of the sound sources is achieved by exploiting a rotational movement which amplifies intensity differences between the two sound sensors.

1 Introduction

In recent years, various types of agent-based simulation models have been employed to look at issues concerning communication in natural organisms and human language which can hardly be investigated with classic analytical models [3, 14]. With respect to analytical and other simulation models, agent-based models do not require the designer to make strong assumptions about the essential features on which social interactions are based—e.g, assumptions concerning what communication is and about the requirement of individual competences in the domain of categorisation and naming. This is particularly true in models in which evolutionary computation algorithms are used to design artificial neural networks as agent’s controllers. These models appear to be a valuable tool to study how semantics and syntax originate from the evolutionary and ontogenetic history of populations of autonomous agents [10, 2]. In other words, the question is how the evolution and the development of perceptual, cognitive and motor capabilities relates to the emergence of a communicative system and possibly language in a population of agents.

By using evolutionary computation and neural network controllers, Tuci et al. [12] described an agent-based model which shows that communication, based on a simple sound signalling system and infrared sensors, evolves in a group of physically different robots required to cooperate in order to achieve a common goal. This paper complements the results and analysis shown in [12] by describing operational aspects of the communication system employed by the robots to perform that task. The experiment we considered is the following: three robots are placed in an arena, as shown in Figure 1. The arena is composed of walls and a light that is always turned on. The light can be situated at the bottom left corridor (*Env. L*) or at the bottom right corridor (*Env. R*). The robots are initialised with their centre anywhere on an imaginary circle of radius 12 cm centred in the middle of the top corridor, at a minimum distance of 3 cm from each other. Their

initial orientation is always pointing towards the centroid of the group. By centroid we refer to the geometric centroid of the triangle formed by the centres of the three robots. The goal of the robots is to (i) navigate towards the light whose position changes according to the type of environment they are situated in, and (ii) avoid collisions.

The peculiarity of the task lies in the fact that the robots are equipped with different sets of sensors. In particular, two robots are equipped with infrared and sound sensors but they have no ambient light sensors. These robots are referred to as R_{IR} (see Figure 2a). The other robot is equipped with ambient light and sound sensors but it has no infrared sensors. We refer to this robot as R_{AL} (see Figure 2b). Robots R_{IR} can perceive the walls and other agents through infrared sensors, while the robot R_{AL} can perceive the light. Therefore, given the nature of the task, the robots are forced to cooperate in order to accomplish their goal. In principle, it would be infeasible for each of them to solve the task solely based on their own perception of the world. R_{AL} can hardly avoid collisions; R_{IR} can hardly find the light source. Thus, the task requires cooperation and coordination of actions between the different types of robots. Notice that the reason why we chose the group to be composed of two R_{IR} and one R_{AL} robot is that this intuitively seems to be the smallest group capable of spatially arranging itself adaptively in order to successfully navigate the world. Although the robots differ with respect to their sensory capabilities, they are homogeneous with respect to their controllers. That is, the same controller, synthesised by artificial evolution, is cloned in each member of the group. Both types of robots are equipped with a sound signalling system (more details in Section 1.1). However, contrary to other studies (see [6, 1]) we do not assume that the agents are capable of distinguishing their own sound from that of the other agents. The sound broadcasted into the environment is perceived by the agent through omnidirectional microphones. Therefore, acoustic signalling is subject to problems such as the distinction between own sound from those of others and the mutual interference due to lack of turn-taking (see [9]).

The goal of this paper is to try to reveal operational aspects of the communication system (e.g., causal relationships between sound signals and behaviour) used by the robots (i) to remain close to the others without colliding, and (ii) to make actions which bring the group closer to the target.

1.1 The simulated agents

The controllers are evolved in a simulation environment which models some of the hardware characteristics of the real *s-bots*. The *s-bots* are small wheeled cylindrical robots, 5.8 cm of radius, equipped with a variety of sensors, and whose mobility is ensured by a differential drive system (see [8] for details). Robot R_{IR} makes use of 12 out of 15 infrared sensors (IR_i) of an *s-bot*, while robot R_{AL} uses the ambient light sensors (AL_1) and (AL_2) positioned at $\pm 67.5^\circ$ with respect to the orientation of the robot (see Figure 2a and 2b). The signal of the infrared sensor is a function of the distance between the robot and the obstacle. Light sensor values are simulated through a

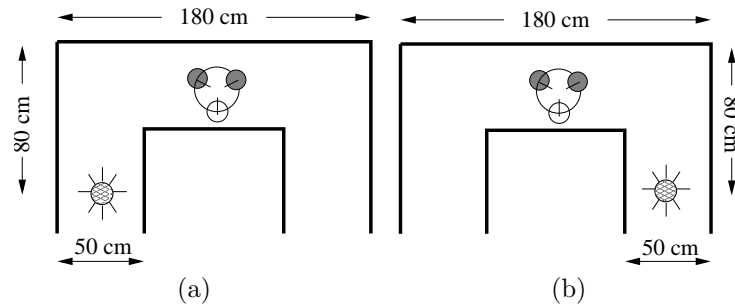


Figure 1: (a) *Env. L*; (b) *Env. R*. The white circle represents robot R_{AL} and the grey circles represent the robots R_{IR} . The thick lines represent the walls, and the filled circles with spikes at the bottom left and right represents the light in each environment.

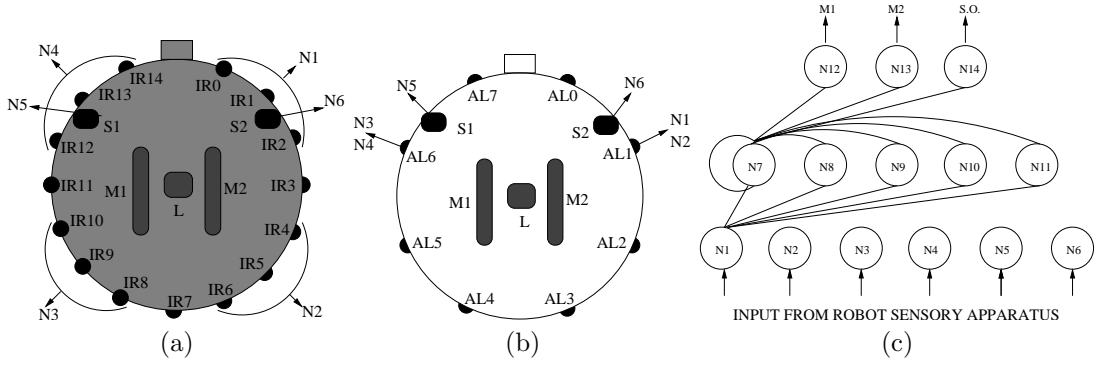


Figure 2: (a) The simulated robots R_{IR} ; (b) The simulated robots R_{AL} ; (c) the network architecture. Only the connections for one neuron of each layer are drawn. The input layer of R_{IR} takes readings as follows: neuron N_1 takes input from the infrared sensors $\frac{IR_0+IR_1+IR_2}{3}$, N_2 from $\frac{IR_4+IR_5+IR_6}{3}$, N_3 from $\frac{IR_8+IR_9+IR_{10}}{3}$, N_4 from $\frac{IR_{12}+IR_{13}+IR_{14}}{3}$, N_5 from sound sensor S_1 , and N_6 from sound sensor S_2 . The input layer of R_{AL} takes readings as follows: N_1 and N_2 take input from ambient light sensors AL_1 , N_3 and N_4 take input from AL_2 , N_5 from S_1 , and N_6 from S_2 . M_1 and M_2 are respectively the left and right motor. L is the loud-speaker (i.e., the sound organ).

sampling technique (see [7]).

All robots are equipped with a loud-speaker (L) that is situated in the centre of the body of the robot, and with two omnidirectional microphones (S_1 and S_2), placed at $\pm 45^\circ$ with respect to the robot's heading. Sound is modelled as an instantaneous, additive field of single frequency with time-varying intensity ($\eta_i \in [0.0, 1.0]$) which decreases with the square of the distance from the source, as previously modelled in [9]. Sound intensity is regulated by the firing rate of neuron N_{14} (see Section 2 for details). Robots can perceive signals emitted by themselves and by other agents. The modelling of the perception of sound is inspired by what described in [9]. There is no attenuation of intensity for self-produced signal. The perception of sound emitted by others is affected by a “self-shadowing” mechanism which is modelled as a linear attenuation without refraction, proportional to the distance (δ_{sh}) travelled by the signal within the body of the receiver

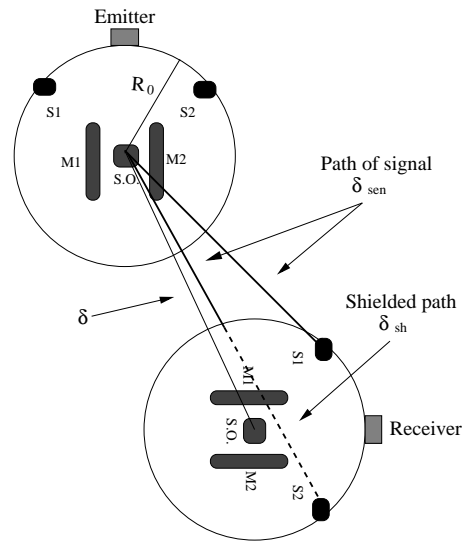


Figure 3: This picture has been adapted from [9]. It shows the working principles of the self-shadowing mechanism.

(see [9] for details). This distance is computed as follows:

$$\delta_{sh} = \delta_{sen}(1 - A), \quad 0 \leq A < 1, \quad A = \frac{\delta^2 - R^2}{\delta_{sen}^2} \quad (1)$$

where δ_{sen} is the distance between the sound source and the sensor and δ is the distance between the sound source and the centre of the body of the receiver, and R is the robot's radius (see also Figure 3). The “self” component of the sound signal is simply equal to η_i . In order to calculate the “non-self” component, we firstly scale the intensity of sound emitted by the sender (η_j) by applying the inverse square law with respect to the distance between the sound source and the microphones of the receiver. Subsequently, we multiply the scaled intensity with an attenuation factor ψ which ranges linearly from 1 when $\delta_{sh} = 0$ to 0.1 when $\delta_{sh} = 2R$. To summarise, the reading \hat{S}_{is} of each sound sensor s of robot i is computed as follows:

$$\hat{S}_{is} = \text{self} + \text{non-self}; \quad \begin{array}{l} \text{self} = \eta_i \\ \text{non-self} = \sum_{\substack{j \in [1,3] \\ j \neq i}} \eta_j \frac{R^2}{\delta_{sen}^2} \psi \end{array} \quad (2)$$

The auditory receptive field of each microphone is bounded within the following interval $\hat{S}_{is} \in [0, 1]$. Therefore, the sound receptor can be saturated by the “self” emitted sound in case a robot emits at its highest intensity ($\eta_i = 1.0$). If the sound sensor is saturated by the “self” component, it is not possible for this robot to perceive sound signals emitted by others. Concerning the function that updates the position of the robots within the environment, we employed the Differential Drive Kinematics equations, as presented in [4]. 10% uniform noise was added to all sensor readings, the motor outputs and the position of the robot. The characteristics of the agent-environment model are explained in detail in [13].

2 The controller and the evolutionary algorithm

The agent controller is composed of a network of five inter-neurons and an arrangement of six sensory neurons and three output neurons (see Figure 2c). The sensory neurons receive input from the agent sensory apparatus. Thus, for robots R_{IR} , the network receives the readings from the infrared and sound sensors. For robots R_{AL} , the network receives the readings from the ambient-light and sound sensors. The inter-neuron network (from N_7 to N_{11}) is fully connected. Additionally, each inter-neuron receives one incoming synapse from each sensory neuron. Each output neuron (from N_{12} to N_{14}) receives one incoming synapse from each inter-neuron. There are no direct connections between sensory and output neurons. The network neurons are governed by the following state equation:

$$\frac{dy_i}{dt} = \begin{cases} \frac{1}{\tau_i}(-y_i + gI_i) & i \in [1, 6] \\ \frac{1}{\tau_i} \left(-y_i + \sum_{j=1}^k \omega_{ji} \sigma(y_j + \beta_j) + gI_i \right) & i \in [7, 14]; \sigma(x) = \frac{1}{1+e^{-x}} \end{cases} \quad (3)$$

where, using terms derived from an analogy with real neurons, y_i represents the cell potential, τ_i the decay constant, g is a gain factor, I_i the intensity of the sensory perturbation on sensory neuron i , ω_{ji} the strength of the synaptic connection from neuron j to neuron i , β_j the bias term, $\sigma(y_j + \beta_j)$ the firing rate. The cell potentials y_i of the 12th and the 13th neuron, mapped into $[0, 1]$ by a sigmoid function σ and then linearly scaled into $[-6.5, 6.5]$, set the robot motors output. The cell potential y_i of the 14th neuron, mapped into $[0, 1]$ by a sigmoid function σ , is used by the robot to control the intensity of the sound emitted η . The following parameters are genetically encoded: (i) the strength of synaptic connections ω_{ji} ; (ii) the decay constant τ_i of the inter-neurons and of neuron N_{14} ; (iii) the bias term β_j of the sensory neurons, of the inter-neurons, and of the neuron N_{14} . The decay constant τ_i of the sensory neurons and of the output neurons N_{12} and N_{13} are set to 0.1. Cell potentials are set to 0 any time the network is initialised or reset, and circuits are integrated using the forward Euler method with an integration step-size of $dt = 0.1$.

A simple generational genetic algorithm is employed to set the parameters of the networks [5]. The population contains 80 genotypes. Generations following the first one are produced by a combination of selection with elitism, recombination and mutation. More details on the characteristics of the evolutionary algorithm employed and on the genotypes' component values can be found in [12].

3 The fitness function

During evolution, each genotype is translated into a robot controller, and cloned in each agent. Then, the group is evaluated eight times, four trials in *Env. L*, and four trials in *Env. R*. The sequence order of environments within the eight trials has no bearing on the overall performance of the group since each robot controller is reset at the beginning of each trial. Each trial (e) differs from the others in the initialisation of the random number generator, which influences the robots' starting position and orientation, and the noise added to motors and sensors. Within a trial, the robot life-span is 400 s (4000 simulation cycles). In each trial, the group is rewarded by an evaluation function f_e which seeks to assess the ability of the team to approach the light bulb, while avoiding collisions and staying within the range of the robots' infrared sensors.

Taking inspiration from the work of Quinn et al. [11], the fitness score is computed as follows:

$$f_e = KP \sum_{t=i}^T [(d_t - D_{t-1})(\tanh(S_t/\rho))]; \quad (4)$$

The simulation time steps are indexed by t and T is the index of the final time step of the trial. d_t is the Euclidean distance between the group location at time step t and its location at time step $t = 0$, and D_{t-1} is the largest value that d_t has attained prior to time step t . S_t is a measure of the team's dispersal beyond the infrared sensor range $\rho = 24.6$ cm at time step t . If each robot is within ρ range of at least another, then $S_t = 0$. Otherwise, the two shortest lines that can connect all three robots are found and S_t is the distance by which the longest of these exceeds ρ .

$P = 1 - \sum_{i=1}^3 c_i/c_{max}$ if $\sum_{i=1}^3 c_i \leq c_{max}$ reduces the score in proportion to the number of collisions which have occurred during the trial. c_i is the number of collisions of the robot i and $c_{max} = 4$ is the maximum number of collisions allowed. $P = 0$ if $\sum_{i=1}^3 c_i > c_{max}$. The team's accumulated score is multiplied by $K = 3.0$ if the group moved towards the light bulb, otherwise $K = 1.0$. Note that a trial was terminated early if (a) the team reached the light bulb (b) the team distance from the light bulb exceeded an arbitrary limit set to 140 cm, or (c) the team exceeded the maximum number of allowed collisions c_{max} . More details on the characteristics of the fitness function can be found in [12].

4 Results

Ten evolutionary simulations, each using a different random initialisation, were run for between 2500 and 3600 generations of the evolutionary algorithm. The termination criterion for each run was set to a time equal to 86400 seconds of CPU time. Experiments were performed on a cluster of 32 nodes, each with 2 AMD Opteron244TM CPU running GNU/Linux Debian 3.0 OS. Recall that the robots of a successful group should be capable of coordinating their movement and of cooperating, in order to approach the target without collisions. A trial is successfully terminated when the centroid of the group is closer than 10 cm to the the light bulb. Cooperation is required since no robot of the group can potentially acquire, through its sensors, sufficient "knowledge" of the environment to accomplish the task. The results of these simulations and of some preliminary post-evaluation tests are illustrated and discussed in [12]. To summarise, we post-evaluated each of the best evolved controllers at the last generation of each evolutionary run. Two of them had a

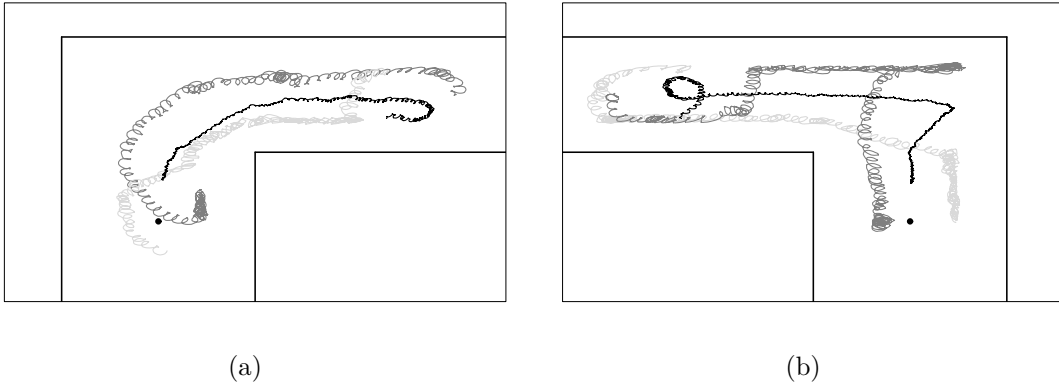


Figure 4: Trajectories of the agents during a successful trial (a) in an *Env. L*, and (b) in an *Env. R*. The black lines refer to the trajectories of robot R_{AL} while the other lines refer to the trajectories of robots R_{IR} . The horizontal and vertical segments represent the walls. In each figure, we depict only the side of the corridor where the light—i.e., the small black dot—is located.

success rate higher than 90% in both environments; two displayed a performance over 80%, while the performance of the remaining six controllers was not sufficiently good in both environments. This paper complements these results by providing an operational analysis of the system, in terms of the mechanisms employed by the robots to achieve their goal. In particular, we focus on the analysis of the behaviour of a group controlled by the best evolved controller run n. 9, that, at the re-evaluation test, had a success rate higher than 90% in both environments.

For the sake of clarity, we recall that during a post-evaluation test, the group is subject to a set of 1200 trials in both environments. The number of post-evaluation trials per type of environment (i.e., 1200) is given by systematically varying the initial positions of the three robots according to the criteria illustrated in [12]. During post-evaluation, the robot life-span is more than two times longer than during evolution (i.e., 1000 s, 10000 simulation cycles). This should give the robots enough time to compensate for possible disruptive effects induced by initial positions never or very rarely experienced during evolution. At the beginning of each post-evaluation trial, the controllers are reset (see Section 2). All the post-evaluation tests illustrated in this paper are carried out by following the criteria mentioned above and detailed in [12]. In all the tests in which different types of alterations are applied to the system to disclose operational principles, the disruptions are applied after 10 s (i.e., 100 simulation cycles) from the beginning of each trial. This should give time to the controllers to reach a functional state different from the initial one, arbitrarily chosen by the experimenter, in which the cell potential of the neurons is set to 0.

4.1 The group’s behaviour

In this section we provide a qualitative description of the individual and group motion of the best evolved simulated agents as observed through a simple graphical interface. First of all, we noticed that the systematic variation of the initial positions of the robots during post-evaluation brings about contingencies in which the coordination of movements of the group toward the target requires an initial effort of the robots in re-arranging their relative positions. During this initial phase of a trial a dynamic process guided by the nature of the flow of sensation (i.e., infrared sensors reading versus ambient light reading) induces the specialisation of the controllers with respect to the physical characteristics of the robots, and to the relative role that they play in the group. This phase is followed by the navigation phase in which the group seems to maintain a rather regular spatial configuration; that is, the two robots R_{IR} place themselves in between the target and the robot R_{AL} . However, note that while *Env. L* requires the group to make a left

turn, *Env. R* requires the group to make a right turn. This asymmetry in the environmental structures corresponds to differences in behavioural strategies employed by the group to reach the target as shown in Figure 4. While in *Env. L* the robots simply turn towards the light keeping their relative positions in the group, in *Env. R* we firstly observe an alignment of the agents along the far right wall (see Figure 4b). Subsequently, the agent close to the corner (see the dark gray line) overcomes the other two and the group starts moving towards the target once the classical configuration of the two robots R_{IR} in between the target and the robot R_{AL} is re-established.

Another important qualitative element is that each of the members of the group is characterised by a movement with a strong angular component (anti-clockwise). In other words, the robots proceed toward the light by rotating on the spot. The evolution of the rotational movement is not particularly surprising if we think about its effect of the perception of sound. First of all, we should remind the reader that the intensity of sound perceived at each microphone results from the summation of two components—the “self” and the “non-self”—and the noise. The “self” component (i.e., the agent’s own signal) is only determined by the intensity of the sound emitted by the robot itself. The “non-self” component is determined by the intensity at which the sound is emitted from the loud-speaker of a sender as well as by the relative distance and orientation of the loud-speaker with respect to the receiver’s microphones. Although the agents have no means to distinguish between the “self” and “non-self” component of the perceived sound, they can act in a way to determine patterns in the flow of sensations which are informative on their spatial relationships. In particular, spatial discrimination of sound sources can be achieved by the receiver through intensity differences between the sound perceived in each ear. In our model, these differences come about from the “simulated” physics of the propagation of sound, including the shadowing effect (see Section 1.1). The rotational movement may introduce rhythm in perception of an amplitude bigger than the oscillations manifested in signalling behaviour. The oscillations of perceived sound, amplified by the rotational movement, may provide the robots the cues to adjust their positions relative to each other, since intensity differences between the two microphones can be a valuable mechanism for spatial discrimination of sound sources. This issue will be extensively investigated in the next section. Notice that, within a trial, pure linear movement replaces the rotational behaviour only sporadically and for a very short interval. This can happen to avoid an imminent danger of collision or if required by the navigational strategy of the group.

Two of the phenomena above mentioned (i.e., the effect of the starting position and the rotational movement) have a strong effect on the time it takes to the group to reach the target. Indeed, as resulted from the post-evaluation test shown in [12], most of the successful trials of the best evolved group of robots last longer than the 400 s given to the groups to complete the task during the evolutionary phase. In the following, we try to clarify the role of sound signalling for the achievement of the group phototaxis and collision avoidance behaviour.

4.2 Coordinated motion through sound signalling

Each robot of the group is required to coordinate its actions in order (i) to remain close to the other two agents without incurring into collisions, and (ii) to make actions which bring the group closer to the target. How are these two objectives achieved? An answer to this question may be provided by showing the relationship between the sensor readings and the actions they trigger in the robots. How the robots sensations influence the way in which they move? In this section we focus on the analysis of the role of the sound with respect to the achievement of the group’s coordination of motion. In Table 1 the reader can find some statistics concerning the intensity of “self” and “non-self” component of the sound as perceived by each agent through its microphones. This Table shows that on average more than 92% of the sound perceived by each agent comes from the “self” component (see Table 1 columns 2 and 8). Moreover, the small standard deviation suggests that each agent is emitting sound at a rather fixed intensity with very small oscillations that are not enough to saturate the auditory channels (see Table 1 columns 3 and 9). Given the high intensity of the “self” component, the “non-self” component can only induce changes in the perception of sound that are less than 1% of the sensors’ receptive-field. However, by looking at the average intensity of the “non-self” component (see Table 1 columns 4, 6, 10, and 12) we

notice that, the latter is already very “weak”, possible due to the relatively “long” robot-robot distances. Despite this, we noticed that, if not affected by the shadowing effect, the “non-self” plus the “self” component may be sufficient to saturate the sensors’ receptive field of the receiver. If we combine this data with the fact that the robots rotate on the spot while moving towards the target, we may deduce that, during navigation, the readings of the sound sensors of each robot may go through oscillations constrained between an upper and a lower bound. The upper bound corresponds to the saturation value (1.0) that is reached when the “non-self” component is not attenuated by the shadowing effect. The lower bound corresponds to the intensity of the “self” component that is reached when the “non-self” component is strongly attenuated by the shadowing effect. These oscillations are very small since they concern less than 1% of the auditory receptive field, and certainly not very regular since the random noise applied to the sensors reading may be large enough to disrupt the regularity of the oscillations determined by the contingencies. However, in spite of being small and noisy, these oscillations seem to be the only phenomenon related to the perception of sound that may play a significant role in the coordination of action of the group. In fact, given a controller sufficiently sensitive to capture them, they may represent a valuable perceptive cue for the receiver to spatially discriminate sound sources and consequently relative position and orientation of the emitter/s. Our hypothesis is that this phenomenon is exploited by the robots to remain close to each other while avoiding collisions and moving towards the target. The tests that follow further investigate our hypothesis on the significance of sound for spatial discrimination and coordination of actions. We run two series of post-evaluation tests. In the first series, we interfere with the propagation of sound in the environment by disrupting the orientation of the robot emitter with respect to the heading of the receiver. We refer to this as the *orientation test*. In the second series, we interfere with the propagation of sound in the environment by disrupting the the sender-receiver distance. We refer to this as the *distance test*. In each of these tests, the robots undergo a set of 1200 trials in each type of environment. For all the simulation cycles following the first 10 seconds of each trial, the sound sensors reading of each agent are computed with respect to a hypothetical state of the system in which the senders are supposed to be:

orientation test: re-oriented by a fixed angular displacement, ranging from a minimum of 18° to a maximum of 180° , with a randomly chosen direction (clockwise or anti-clockwise) with respect to the heading of the receiver.

distance test: at a fixed distance to the receiver, ranging from a minimum of 2 cm to a maximum of 32 cm.

Note that, the hypothetical states are taken into account only as far as it concerns the updating of the sound sensors’ reading of one type of robot at the time. That is, during a set of trials, the sound perceived by robot R_{AL} is computed with reference to a hypothetical state in which the orientation/position of both robots R_{IR} is changed in order to meet the angular displacement/distance requirements. In this type of tests no disruptions are applied to update the sound

Table 1: This table shows average and standard deviation of the “self” and “non-self” component of the intensity of the sound perceived by the robots at each of their microphone— $S1$ and $S2$ —during 1200 trials in each environment. Recall that the “self” component does not differ between the microphones of the emitter.

	<i>Env. L</i>						<i>Env. R</i>					
	self		non-self				self		non-self			
			S1		S2				S1		S2	
	avg	std	avg	std	avg	std	avg	std	avg	std	avg	std
R_{IR}	0.935	0.027	0.059	0.0574	0.054	0.046	0.936	0.028	0.067	0.063	0.060	0.048
R_{IR}	0.934	0.028	0.063	0.061	0.0571	0.047	0.936	0.028	0.064	0.062	0.0571	0.048
R_{AL}	0.925	0.012	0.061	0.058	0.061	0.055	0.922	0.017	0.063	0.059	0.063	0.059

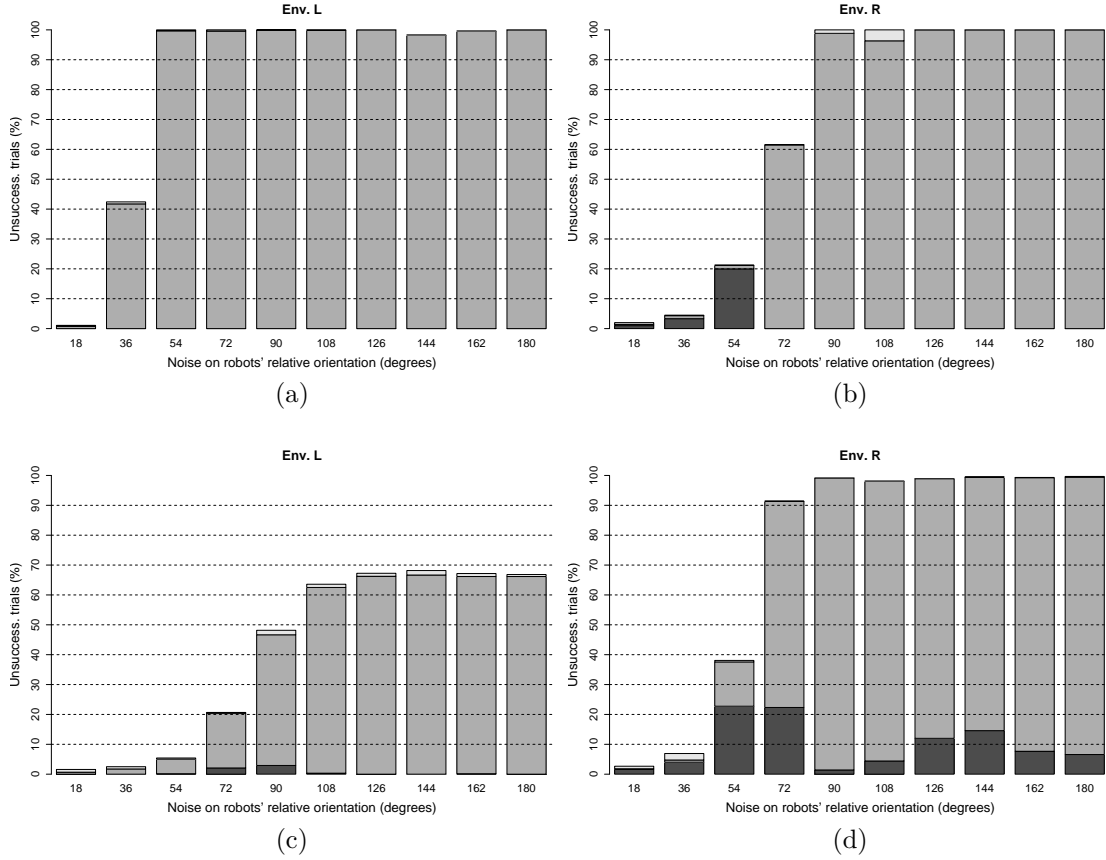


Figure 5: Percentage of failure during 1200 trials in each type of environment in post-evaluation tests with alterations applied to the relative orientation of the robots during the computation of the perceived sound. In (a) and (b) the robots R_{IR} , during all the simulation cycles following the first 10 seconds of any trial, are considered to be re-oriented with respect to the heading of robot R_{AL} by applying the angular displacement indicated on the horizontal axis and randomly choosing the direction of displacement (i.e., clockwise or anti-clockwise). In (c) and (d) the robot R_{AL} is re-oriented with respect to the heading of each robot R_{IR} as explained above. (a) and (c) refer to tests in *Env. L*; (b) and (d) refer to tests in *Env. R*. The black area of the bars refers to the percentage of trials terminated without collisions and with the group not having reached the target. The light grey area of the bars refers to the percentage of trials terminated due to robot-robot collisions. The dark grey area of the bars refers to the percentage of trials terminated due to robot-wall collisions.

perceived by robots R_{IR} . For the *orientation test* the results are shown in Figure 5a and 5b. For the *distance test*, the results are shown in Figure 6a and 6b. In a different set of tests, the sound perceived by the robots R_{IR} is computed with reference to a hypothetical state in which the orientation/position of robot R_{AL} is changed in order to meet the angular displacement/distance requirements. In this type of tests no disruptions are applied to update the sound perceived by robot R_{AL} . For the *orientation tests* the results are shown in Figure 5c and 5d. For the *distance test*, the results are shown in Figure 6c and 6d.

Generally speaking, by varying the sender-receiver orientation/distance, we indirectly increase/decrease the magnitude of the “non-self” component. In particular, those hypothetical states in which the sender-receiver distances tend to be decreased with respect to normal conditions, produced an increase of the magnitude of the “non-self” component and consequently an

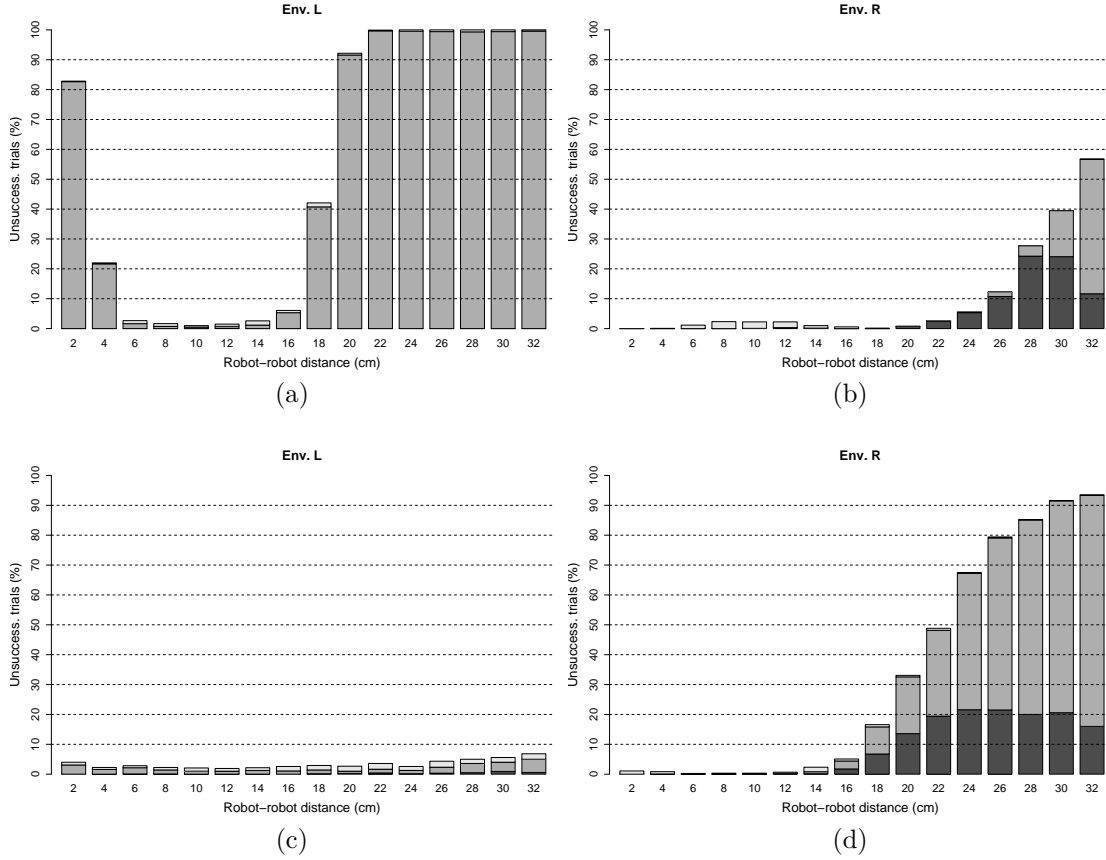


Figure 6: Percentage of failure during 1200 trials in each type of environment in post-evaluation tests with alterations applied to the robot-robot distance during the computation of the sound perceived by the receiver. In (a) and (b) the robots R_{IR} , during all the simulation cycles following the first 10 seconds of any trial, are both considered to be at the distance to robot R_{AL} indicated on the horizontal axis. In (c) and (d) the robot R_{AL} is considered to be at the distance to robots R_{IR} indicated on the horizontal axis as explained above. (a) and (c) refer to tests in *Env. L*; (b) and (d) refer to tests in *Env. R*. The black area of the bars refers to the percentage of trials terminated without collisions and with the group not having reached the target. The light grey area of the bars refers to the percentage of trials terminated due to robot-robot collisions. The dark grey area of the bars refers to the percentage of trials terminated due to robot-wall collisions.

increase of the proportion of time in a trial the sound sensors are saturated. The same effect is obtained by applying angular displacements which increase the attenuation factor ψ . On the contrary, those hypothetical states in which the sender-receiver distances tend to be increased, produce a decrease of the magnitude of the “non-self” component and consequently a decrease of the proportion of time in a trial the sound sensors are saturated. The same effect is obtained by applying angular displacements which decrease the attenuation factor ψ . However, while the *distance test* preserves the intensity differences between the sound perceived in each ear due to the relative orientation of the sender with respect to the receiver, the *orientation test* disrupts any kind of regularities in the perception of sound which are linked to sender-receiver relative orientation. Therefore, a drop in performance at the *orientation test* can be a sign of the significance of binaural perception for spatial discrimination and behavioural coordination. Contrary to the *orientation test*, the *distance test* informs us on the robustness of the mechanisms that exploit binaural perception with respect to a general increase/decrease of the intensity of the “non-self”

component.

The results of the tests shown in Figure 5 and 6 are very informative. First, the performance of the group is significantly disrupted by alterations which concern the orientation of the sender with respect to the heading of the receiver. Figure 5 shows that the bigger the magnitude of the disruption the higher the percentage of failure of the system. This proves that intensity differences between the sound perceived in each ear have a bearing on the development of effective navigational strategies as hypothesised above. In particular, regularities in the oscillation of the sound sensors' reading linked to the environmental contingencies and to the "variation" of the "non-self" component, are important perceptual cues exploited by the agents to coordinate their movements. The majority of failure are due to robot-wall collision. In particular, by looking at the behaviour of the group in these conditions, we noticed that, under the effects induced by the disruptions, the robots are not capable of remaining close to each other—i.e., within the infrared sensors' range. When the distances becomes too high, the robots start wandering around the arena, and the trial terminates due to a collision of the robot R_{AL} with the arena walls. Only in few circumstances the robots do not lose contact to each other but they are not capable of reaching the target within the time-limits (see Figure 5 black area of the bars).

The results shown in Figure 6 tell us that the mechanisms which exploit binaural perception for spatial discrimination and behavioural coordination are quite robust to a general increment of the sound intensity. An exception is the case in which the robots R_{IR} are placed very close to robot R_{AL} in an environment *Env. L* (see Figure 6a). By looking at the behaviour of the group in these conditions, we noticed that contrary to what observed in the *orientation test*, in the unsuccessful trial the robots manage to remain close to each other—i.e., within the infrared sensors' range. However, the robot R_{AL} is not capable of making the left turn hitting the walls close to the corner. This is a quite general problem in these type of tests. That is, the robots manage to approach the turn (left or right) relatively close to each other but they fail due to the lack of behavioural coordination of robot R_{AL} during the turn. Another significant result is that the robustness with respect to this type of disruptions is not the same for both types of robots. In general, the most disruptive effects are recorded in those tests in which discrepancies are artificially induced between the current state of the system and the perception of sound of robot R_{AL} . Disruptions on the perception of sound of robots R_{IR} when the group is located in *Env. L* do not alter the performance of the system with respect to the normal conditions (see Figure 6c). This suggests that, in *Env. L* robots R_{IR} "favour" infrared over sound sensors to coordinate their actions.

5 Conclusion

The paper described operational aspects of the behaviour of a group of robots equipped with a different set of sensors, that navigates towards a target in a walled arena. The results of our analysis suggest that the robots use sound to regulate the inter-robot distances. Movements towards a zone of higher/lower intensity of sound keep the robots close to each other at a safe distance. The robots R_{IR} tend to place themselves in between the robot R_{AL} and the target. Owing to this spatial displacement, the motion toward the target of robot R_{AL} is secured from collision against the walls. Rotational movement introduces rhythm in perception which is an important cue to spatially discriminate the sound source. Implementation details, such as the homogeneity of the controllers, or the mechanism employed to regulate the sound intensity, may have precluded our system the possibility to develop a more articulated signalling behaviour. Future work will explore solutions that allow the agents to develop more complex communication through mechanisms which favour the recognition of "self/non-self" sound, and help minimise the interference between simultaneous production.

6 Acknowledgements

E. Tuci and M. Dorigo acknowledge European Commission support via the *ECAgents* project, funded by the Future and Emerging Technologies programme (grant IST-1940), and by COMP2SYS, a Marie Curie Early Stage Training Site (grant MEST-CT-2004505079). The authors thank their colleagues at IRIDIA for stimulating discussions and feedback during the preparation of this paper, and the two anonymous reviewers for their helpful comments. M. Dorigo acknowledges support from the Belgian FNRS, of which he is a Research Director, and from the “ANTS” project, an “Action de Recherche Concertée” funded by the Scientific Research Directorate of the French Community of Belgium. The information provided is the sole responsibility of the authors and does not reflect the Community’s opinion. The Community is not responsible for any use that might be made of data appearing in this publication.

References

- [1] G. Baldassarre and S. Nolfi and D. Parisi. Evolving mobile robots able to display collective behaviour. *Artificial Life*, 9:255–267, 2003.
- [2] A. Cangelosi. Approaches to grounding symbols in perceptual and sensorimotor categories. In H. Cohen and C. Lefebvre, editors, *Handbook of Categorization in Cognitive Science*, pages 719–737. Elsevier, 2005.
- [3] A. Cangelosi and D. Parisi, editors. *Simulating the Evolution of Language*. Springer Verlag, London, UK, 2002.
- [4] G. Dudek and M. Jenkin. *Computational Principles of Mobile Robotics*. Cambridge University Press, Cambridge, UK, 2000.
- [5] D. E. Goldberg. *Genetic Algorithms in Search, Optimization and Machine Learning*. Addison-Wesley, Reading, MA, 1989.
- [6] D. Marocco and S. Nolfi. Emergence of communication in embodied agents: Co-adapting communicative and non-communicative behaviours. In A. Cangelosi, G. Bugmann, and R. Borisjuk, editors, *Modeling language, cognition and action: 9th Neural Computation and Psychology Workshop*. World Scientific, 2005.
- [7] O. Miglino, H.H. Lund, and S. Nolfi. Evolving mobile robots in simulated and real environments. *Artificial Life*, 2(4):417–434, 1995.
- [8] F. Mondada, G. Pettinaro, A. Guignard, I. Kwee, D. Floreano, J.-L. Deneubourg, S. Nolfi, L. Gambardella, and M. Dorigo. SWARM-BOT: A new distributed robotic concept. *Autonomous Robots*, 17(2–3):193–221, 2004.
- [9] E. Di Paolo. Behavioral coordination, structural congruence and entrainment in a simulation of acoustically coupled agents. *Adaptive Behavior*, 8(1):27–48, 2000.
- [10] M. Quinn. Evolving communication without dedicated communication channels. In J. Kelemen and P. Sosik, editors, *Advances in Artificial Life: 6th European Conf. on Artificial Life*, pages 357–366. Springer Verlag, Berlin, Germany, 2001.
- [11] M. Quinn, L. Smith, G. Mayley, and P. Husbands. Evolving controllers for a homogeneous system of physical robots: Structured cooperation with minimal sensors. *Phil. Trans. of the Royal Soc. of London, Series A*, 361:2321–2344, 2003.
- [12] E. Tuci, C. Ampatzis F. Vicentini, and M. Dorigo. Evolved homogeneous neuro-controllers for robots with different sensory capabilities: coordinated motion and cooperation. Technical Report TR/IRIDIA/2006-015, IRIDIA, Université Libre de Bruxelles, May 2006. Technical report available at <http://iridia.ulb.ac.be/IridiaTrSeries>.

- [13] F. Vicentini and E. Tuci. *Swarmod: a 2d s-bot's simulator*. Technical Report TR/IRIDIA/2006-005, IRIDIA, Université Libre de Bruxelles, 2006. Technical report available at <http://iridia.ulb.ac.be/IridiaTrSeries>.
- [14] P. Vogt. Language acquisition and evolution. *Adaptive Behavior*, 13(4):265–268, 2005.